Implementation of a Digital Image Superposition Algorithm for Radionuclide Images: An Assessment of Its Accuracy and Reproducibility

David L. Williams, James L. Ritchie, and Glen W. Hamilton

Veterans Administration Hospital, Seattle, Washington

An operator-interactive algorithm to achieve superposition of organ images has been used with a dedicated nuclear medicine computer system. Its purpose is to achieve organ registration in 128 × 128 digitized images before a direct numerical comparison of the regional distribution of a deposited radiotracer is performed. The accuracy and reproducibility of the algorithm for myocardial images has been tested by four operators, using a set of 28 image pairs in which the relative position of the heart differed by more than 10 mm for each pair. Comparing their results with the known displacements on two occasions provided an assessment of these two important parameters. The accuracy and reproducibility for superposing myocardial images by this digital technique are found to be well within the spatial resolution (FWHM) of the imaging system for the Tl-201 tracer studied.

J Nucl Med 19: 316–319, 1978

Direct comparison of the in vivo spatial distribution of different radionuclides, or the same radionuclide administered under varying physiologic conditions, is frequently of considerable importance. Typical examples are the combination of Xe-133 ventilation and Tc-99m MAA perfusion lung images (*1–3*) and the rest/exercise Tl-201 myocardial studies (*4,5*). For subjective visual interpretation, exact image registration or superposition is usually not necessary.

However, several dual-isotope studies of the heart (*6–8*), lungs (*1–3*), or pancreas (*9,10*) have required precise image registration to perform image subtraction, quantitative comparisons of spatial distributions, and/or simultaneous display of superposed organs by black-and-white or color techniques. Exact image registration is easily obtained in these cases by simultaneously or sequentially recording the scintillation-camera images without moving the patient.

When the images must be obtained at different times (e.g., the rest/exercise Tl-201 myocardial study), accurate image registration is more difficult to obtain. Price et al. have developed digital processing techniques to achieve image superposition. They have considered the most general case in which translations, rotations, magnifications, and distortions exist between two images and have applied their mathematical formulation to Anger camera/rectilinear scanner and Anger camera/x-ray imaging problems (*11,12*). Their applications include computer reconstruction of registered transparent film images of xenon washout parameters and contrast arteriograms for comparison on an x-ray viewbox.

In an effort to develop quantitative methods for the comparison of resting/exercise Tl-201 myocardial images, we have implemented an image superposition algorithm that provides operator-interactive control of the translational orientation of two 128 × 128 digitized images. The program was developed in the assembly language of the Nova-series computers and uses specific attributes of the refreshed-CRT display system of the computer system. Differences in image magnification have not been considered, since high-resolution, parallel-hole collimators were used, and these have constant magnification with distance from the collimator's surface (*13*). Images of superposed organs are stored on computer disk along with the originals so that processing techniques can be applied to determine regional variations.

The image-superposition algorithm. The flow diagram of

Received July 25, 1977; revision accepted Oct. 28, 1977.

For reprints contact: David L. Williams, Nuclear Medicine Sec. (115), Veterans Administration Hospital, 4435 Beacon Ave. S., Seattle, WA 98108.

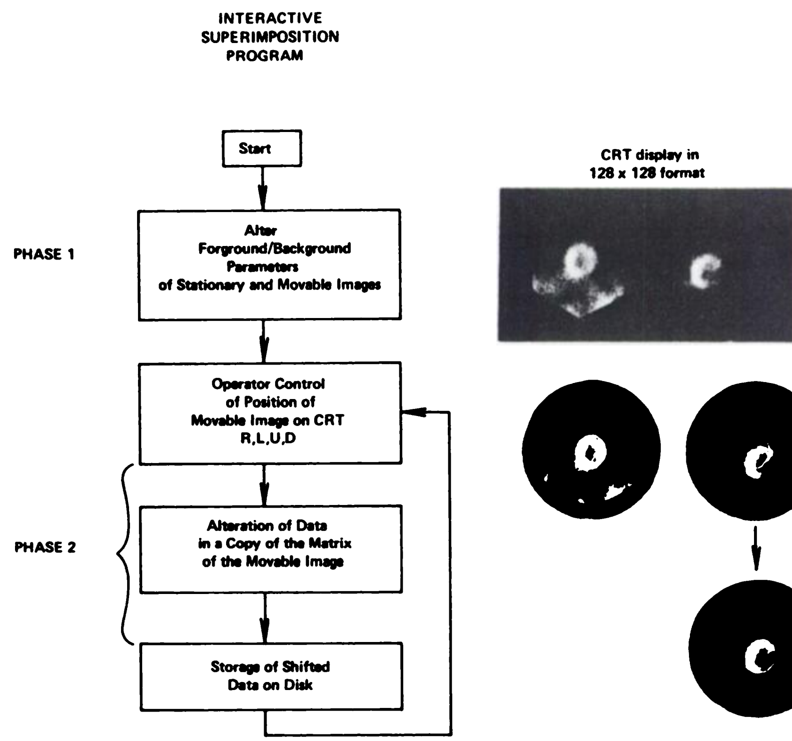

FIG. 1. Block diagram (left) and images (right) summarize operation of image-superposition algorithm. Superposition procedure is carried out in two phases: (a) image enhancement, and (b) image superposition. Clinical example used to illustrate each phase is rest/exercise thallium-201 study in left anterior oblique view, where patient develops large posterior defect on exercise. In phase 1, scintillation camera images are read from disk and displayed (with no image enhancement in this example). In phase 2, the exercise myocardial image is interactively superimposed upon the rest image with subsequent alteration of digital matrix data so that quantitative spatial comparisons can be performed.

the image-superposition program is given in Fig. 1. Program execution occurs in two phases. In Phase One, a stationary 128 × 128 image (SI) and a movable 128 × 128 image (MI) are read from disk and displayed adjacent to one another, as shown in Fig. 1. The operator has interactive control of foreground and background enhancement parameters of each image. The two displays are switched on the CRT rapidly enough so that both images are visible simultaneously. Once satisfied with the enhancement parameters, the operator progresses to superposition mode in Phase Two. Initially, the SI and MI data matrices appear registered along with an optional edge display, which depicts the approximate location of the organ of interest in the SI. Note that either the SI and border display or the MI and border display are visible on the CRT at one time. The movable and stationary image displays are alternately switched on the CRT with a software-controlled persistence time specified by the operator. Simultaneous with this display switching sequence, the operator has keyboard control of the position of the movable image with respect to the stationary image, and can move the MI up, down, to the right or left until organ activity distributions appear in registration. Rapid control over the position of the MI relative to the SI is achieved by altering display parameters rather than image matrix data. The optional border display has been useful to the operator in achieving organ superposition quickly. Once superposition is visually achieved on the CRT, the counting data in the matrix of the MI are shifted according to the current translation specifications, thus producing an output image matrix with organ count data in registration with those in the SI. Data shifting is completed in ½ sec.

Sources of inaccurate image superposition with specific application to Tl-201 myocardial imaging in the left anterior oblique view. The fundamental assumption in the use of digital image superposition is that the organ system of interest maintains a fixed anatomic relationship in both images. In addition, accurate superposition of digitized scintigrams depends upon several factors related to imaging technique and computer analysis. These include (a) detector repositioning in angle, and (b) patient repositioning with respect to rotation in the plane parallel with the collimator's surface, (c) image quantization into a digital matrix, and (d) intra- and inter-operator variability. As the computer algorithm described here does not, at present, permit rotations, the patient must be reproducibly located beneath the scintillation camera's detector with respect to polar and azimuthal angles. The detector-orientation problem is solved by writing into the patient's chart the particular detector angles used during the first clinical study and then reproducing them on subsequent procedures. Relocation in azimuth is accomplished with the aid of an orthogonal coordinate system established on the floor of the imaging room beneath the detector. The patient is placed supine on the imaging table and parallel to its edges. Using the ruled grid, the imaging table is positioned to bring the patient into contact with the collimator's surface while remaining parallel to both axes. Azimuthal reproducibility is estimated to be within 5°.

Uncertainty regarding image quantization depends upon the matrix resolution used for digitizing the image. In each direction there exists a finite distance, D, equal to the matrix spacing, over which position coordinates will be assigned to the same matrix channel. If a known position is repeatedly located with respect to the matrix, its probability for assignment to a given channel is specified by the uniform probability distribution in each orthogonal direction. Figure 2 illustrates this concept for the one-dimensional case. From this distribution, the standard deviation for repeated positioning in one dimension is calculated to be 0.6 mm for our spatial calibration. For the two-dimensional case, the quantizing uncertainty is confined to an area with a radius of 0.9 mm ($0.6 \times \sqrt{2}$). This uncertainty is approximately one-half that due to human operator variability, as will now be discussed.

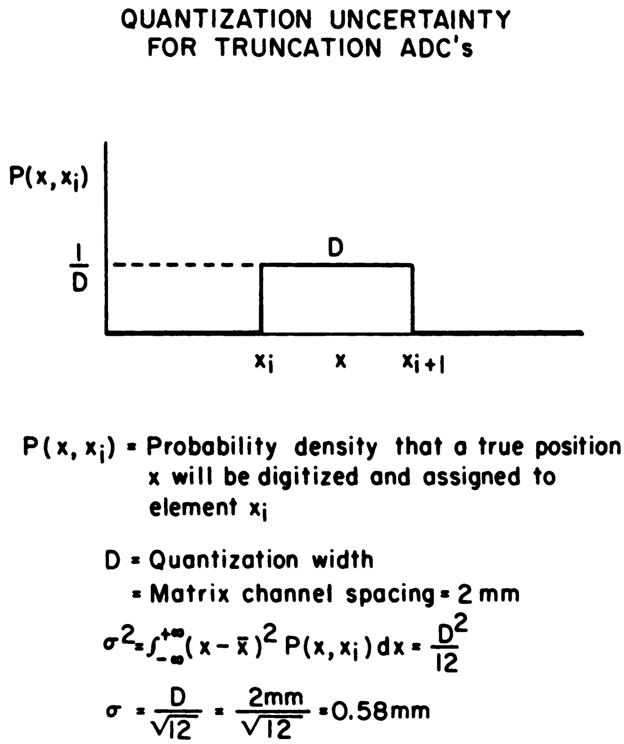

FIG. 2. Probability distribution used for calculating quantization uncertainty. Uniform probability distribution describes probability $P(x,x_i)$, in one dimension, that a true position coordinate x will be digitized into histogram bin x_i. Standard deviation for repeated positioning is calculated from distribution to be 0.58 mm.

The major source of superposition inaccuracy is the operator's visual judgment of organ registration. To evaluate the details of intra- and inter-operator accuracy and reproducibility, we have chosen a specific model that simulates rest/exercise Tl-201 myocardial imaging in the left anterior oblique (LAO) view (*4,5*). Twenty-eight clinical imaging studies were performed in the resting state with 300 K counts per image. They were simultaneously recorded by a scintillation camera and by a dedicated nuclear imaging computer system (MDS). Following completion of the LAO view, a second LAO image was acquired with no change in patient positioning. Each pair of digitized, registered images thus differed only in their random fluctuations, as illustrated in Fig. 3. The second of each pair was subsequently computer-processed to shift its orientation in both X and Y directions from 10 mm to 50 mm away from the point of exact registration, and then saved on disk. The purpose of the shifted second image was to simulate an exercise myocardial image derived at a different time, but containing no intrinsic translational or rotational misalignment with respect to the digital image matrix. The unaltered first image and the shifted second image (Fig. 4) were incorporated into the data set for studying operator accuracy and reproducibility.

One should note three minor differences that distinguish the test data from those acquired in actual clinical Tl-201 rest/exercise imaging procedures. Since the patient was not moved between views, no possibility exists in the test data for inexact positioning in the rotational sense or for difference in the digitization uncertainty. The myocardial-to-background (signal-to-noise) ratio on the second rest image, which simulated the exercise state, was lower than that of a true exercise Tl-201 study (*14*). Approximation of the image-registration problem with only rest images worsens an operator's impression of the myocardial boundary in the simulated exercise image. The reproducibility and accuracy experiment therefore provides worst-case estimates of the human component of a more complex imaging procedure.

Accuracy and reproducibility were assessed by presenting four operators with the 28 image pairs and asking them to place the second (computer-translated) image into registration with the first using the image-superposition program. Each operator repeated the exercise 1 wk later. Cases were mixed randomly between the two studies and identified only by number. For each image pair, the operator recorded the X and Y displacements of the second image for which the best visual registration occurred. The relative translation of the second image could be obtained at any time by a keyboard command to the computer. Displacements for an operator's first run were compared with the known displacements to assess accuracy. Reproducibility was investigated by intercomparing the two runs for the same operator. Results for the accuracy and reproducibility studies are summarized in Tables 1 and 2, respectively.

It is convenient to summarize the results in terms of a root-mean-square (RMS) radius of accuracy and reproducibility for each operator. The RMS accuracy radius is calculated from

$$R_{acc} = [1/28 \sum_{1}^{28} [(X_1 - X_T)^2 + (Y_1 - Y_T)^2]]^{1/2},$$

where the quantities $(X_1 - X_T)$ and $(Y_1 - Y_T)$ measure the differences in X and Y, respectively, between the operator's (X_1, Y_1) and the true displacements (X_T, Y_T) for Run 1. The subscript denoting study number has been omitted from these terms to simplify the notation. Similarly, an RMS reproducibility radius is calculated from

$$R_{rep} = [1/28 \sum_{1}^{28} [(X_1 - X_2)^2 + (Y_1 - Y_2)^2]]^{1/2},$$

where the quantities $(X_1 - X_2)$ and $(Y_1 - Y_2)$ measure the

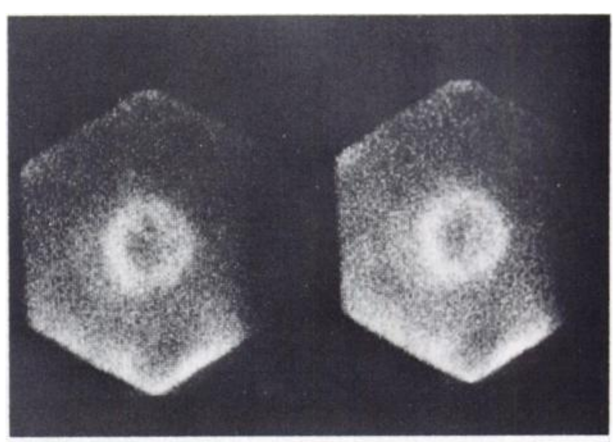

FIG. 3. Image data acquired for purpose of establishing accuracy and reproducibility of operator-interactive digital image-superposition algorithm. Sequential 300,000 count, LAO image pairs of myocardial distribution of thallium-201 in resting state were used as basis for these determinations. Neither patient nor imaging table was moved between the two views. Images differ only in their random fluctuations and uncontrollable patient movement (e.g., respiration).

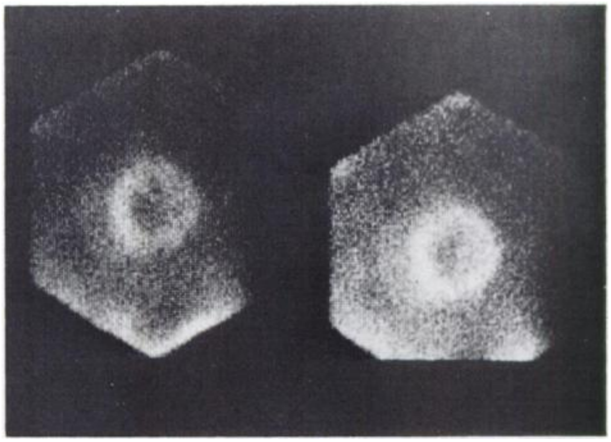

FIG. 4. Typical data set presented to human operators to assess accuracy and reproducibility. Digital data in right-hand panel were produced by displacing second sequential image a known distance (from 10 mm to 50 mm) away from point of exact registration. Shifted second image was used to simulate exercise image acquired on a different day.

TABLE 1. RESULTS OF ACCURACY STUDY

	Operator 1	Operator 2	Operator 3	Operator 4
RMS radius (mm)	2.6	2.3	2.6	2.0

Average RMS accuracy radius for four operators = 2.4 mm.

TABLE 2. RESULTS OF REPRODUCIBILITY STUDY

	Operator 1	Operator 2	Operator 3	Operator 4
RMS radius (mm)	2.6	1.4	2.3	1.3

Average RMS reproducibility radius for four operators = 1.9 mm.

differences between the operator's *X* and *Y* displacements for Runs 1 and 2. The results in Table 1 indicate that the average RMS accuracy radius for the four operators is 2.4 mm and the average RMS reproducibility radius is 1.9 mm. Combining the intrinsic digitizing uncertainty with accuracy or reproducibility uncertainties, we conclude that the overall accuracy for the computer-processing aspects of digital image superposition under the simulated conditions is within a radius of approximately 3 mm. This value is approximately 25% of the spatial resolution in vivo for imaging the 80-keV x-rays from the Tl-201 daughter.

CONCLUSION

A computer program that achieves image superposition of digitized 128 × 128 images by operator interaction has been developed. The algorithm is intended as a preprocessing step in performing quantitative spatial comparisons between two images. The subjective nature of the operator's involvement has been investigated for conditions that simulate rest/exercise Tl-201 myocardial imaging, with the finding that overall accuracy and reproducibility are uncertain within a circle with an RMS radius of about 3 mm in the object plane.

ACKNOWLEDGMENTS

This work was supported by NIH Grant #HL-18805-02 and the General Medical Research Service, Seattle Veterans Administration Hospital.

The authors acknowledge the programming efforts of D. Walter Biggs III, who made significant contributions to this work. We thank our technologists, Ann Coleman and Michael Robertson, for their care in acquiring the clinical data. We also acknowledge the secretarial assistance of Katharine Jelsing and Carol Maurer, and the work of our medical illustrator, Joy Godfrey, and photographer, Clinton Kolyer.

REFERENCES

1. Treves S, Ahnberg DS, Laguarda R, et al: Radionuclide evaluation of regional lung function in children. *J Nucl Med* 15: 582–587, 1974

2. Jacobstein JG: ^{133}Xe ventilation scanning immediately following the ^{99m}Tc perfusion scan. *J Nucl Med* 15: 964–968, 1974

3. Nolan NG: Computer assisted Tc-99m–Xe-133 scintigraphic diagnosis of pulmonary embolism using crossover subtraction. *J Nucl Med* 16: 553, 1975 (abst)

4. Bailey IK, Griffith LSC, Rouleau J, et al: Thallium-201 myocardial perfusion imaging at rest and during exercise: Comparative sensitivity to electrocardiography in coronary artery disease. *Circulation* 55: 79–87, 1977

5. Ritchie JL, Trobaugh GB, Hamilton GW, et al: Myocardial imaging with ^{201}Thallium at rest and during exercise: Comparison with coronary arteriography and resting and stress electrocardiography. *Circulation* 56: 66–71, 1977

6. Ashburn WL, Braunwald E, Simon AL, et al: Myocardial perfusion imaging with radioactive-labeled particles injected directly into the coronary circulation of patients with coronary artery disease. *Circulation* 44: 851–865, 1971

7. Jansen C, Judkins MP, Grames GM, et al: Myocardial perfusion color scintigraphy with MAA. *Radiology* 109: 369–380, 1973

8. Ritchie JL, Hamilton GW, Gould KL, et al: Myocardial imaging with Indium-113m and Technetium-99m macroaggregated albumin. *Am J Cardiol* 35: 380–389, 1975

9. Overton TR, Heslip PG, Barrow PA, et al: Dual-radioisotope techniques and digital image-subtraction methods in pancreas visualization. *J Nucl Med* 12: 493–498, 1971

10. Skretting A: An iterative computer algorithm for optimization of radionuclide subtraction studies. *Phys Med Biol* 20: 578–592, 1975

11. Price RR, Lindstrom S, Hillis GC, et al: Analytical techniques for image superimposition. In *Proceedings of the 5th Symposium on Sharing of Computer Programs and Technology in Nuclear Medicine*, Salt Lake City, 1975, pp 241–250

12. Price RR, Brill AB, Graham T, et al: Analysis of cardiac function and regional myocardial blood flow using radioisotope and radiographic images. In *Information Processing in Scintigraphy*, Orsay, 1975, pp 136–162

13. Harris CC, Satterfield MM, Ross DA, et al: Moving-detector scanners versus stationary imaging devices. In *Fundamental Problems in Scanning*, Gottschalk A and Beck RN, eds. Springfield, Ill., CC Thomas, 1968, pp 93–112

14. Cook DJ, Bailey I, Strauss HW, et al: Thallium-201 for myocardial imaging: Appearance of the normal heart. *J Nucl Med* 17: 583–589, 1976